

Interactive Dynamic Analysis of Subsea Lifting Ropes

George Laird

Predictive Engineering, Inc.

Kirk Fraser

Predictive Engineering, Inc.

Ryan Marsh

Sound Ocean Systems, Inc.

Abstract

The dynamic movement of subsea ropes presents an interesting numerical challenge due to the coupling of drag forces with the dynamic response of the rope. Although a FSI approach of fully coupling the surrounding seawater to the rope is theoretically possible it lies beyond the reach of practical engineering when discussing rope lengths in kilometers and possible rope movements in hundreds of meters. A new analysis technique is presented where the drag forces associated with subsea dynamic rope movement are directly integrated into the solution using the LS-DYNA user subroutine, LOADUD. Drag forces are calculated from analytical solutions to provide discrete drag forces as a function of rope position and velocity. This technique avoids the complexity of a fully-coupled FSI solution while providing the major benefits capturing how the rope will dynamically move while lifting heavy loads while being subjected to strong sea currents. Results are presenting showing how a two kilometer rope would dynamically behave while lifting a heavy load from sea bottom to surface under stratified sea currents.

Introduction

Ropes are everywhere in ocean engineering (see Figure 1). They moor, they lift, they tow, they guide and they act as umbilical's. Their dynamic behavior as influenced by loading and ocean currents is of wide interest and the literature is chock full of studies [1]. A common dynamic problem with tensioned subsea ropes is strumming [2] due to vortex shedding. As a dynamic system, once it starts to excite, failure is not far behind. This rope to fluid dynamic interaction is complex and although a brute force fluid-structure-interface (FSI) is possible, computational difficulties would hinder this approach on the kilometer scale. Approximate FSI solutions are offered in the literature where the surrounding fluid mass is approximated as *added mass* [3] to the dynamic solution but this approach is only relevant when the fluid is quiescent around the rope and obviously fails to capture the dynamic loading due to vortex shedding. Thus, a conundrum exists as to how one could more realistically simulate the dynamic behavior of long rope runs under dynamic loading subjected to varying ocean currents.

Our approach is to idealize the fluid behavior down to its essential mechanical interaction with the rope. We ignore interfacial turbulence and fluid mass coupling to the rope and focus on the transfer of fluid forces to the rope due to vortex shedding and drag. This approach is shown as logical given the characteristics of the rope and its operating conditions. LS-DYNA's ICFD was used to calculate the vortex shedding forces and results were verified against hand calculations. All fluid forces (vortex and drag) were calculated as functions of nodal-specific rope velocity. To obtain the idealized dynamic FSI coupling between the rope and the fluid, a user load (LS-DYNA loadud) routine was developed that would dynamically link the rope movement to the fluid forces. With this loadud routine, the user has customized inputs to account for rope diameter, surface roughness and on the sea side, ocean currents as a function of depth. This loadud routine is coupled to the mechanical model of the rope system.

The mechanical model simulates the heavy-lift operation from deep-ocean environments (>5 km) using large diameter high-modulus polyethylene rope (Spectra). During the lift operation, the rope moves at sufficient velocity that strumming induced by vortex shedding and ocean currents is of real concern. Given that the cost of the rope is in the millions of dollars, the importance of this modeling effort was never in doubt.

This paper provides an overview of the idealization approach to simplify the FSI effects to a basic mechanical coupling that can be incorporated in a LS-DYNA user routine (loadud) to provide real-time dynamic coupling of the complete rope-lift system. Results are presented showing how the system functions and several dead-ends which were discarded due to numerical difficulties.

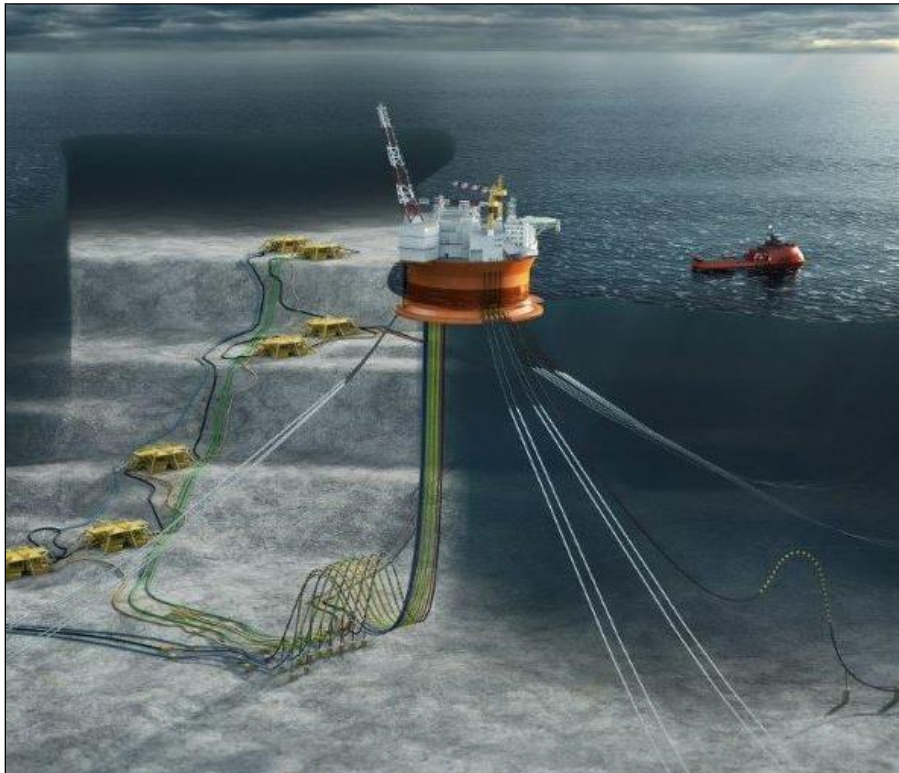


Figure 1 - Examples of how undersea ropes are used

Description of Heavy-Lift Deep-Sea Rope System

The heavy-lift system has a design requirement to reach ocean depths of at least 5 km. Given the heavy loads, the design starts out with a main line diameter of 3.0 inch with a haulback line diameter of 1.0 inch. On the surface, the rope is spooled within large diameter winch drums while on the sea floor, a large diameter pulley is mounted upon a tethered platform.

Figure 2 shows an example of one of the first models that was attempted. To move the rope around the virtual pulleys, the option *ELEMENT_BEAM_PULLEY was employed and then discarded due to unacceptable dynamic noise. The yellow cylinders at the entry/exit points for the pulleys represent where guided contact (*CONTACT_GUIDED_ROPE) was used. This was first of many attempts to create a numerically efficient model. The rationale for this pursuit was the long run times to complete the lift circuit. An implicit solution was considered but given

dynamic time step requirements and the use of contact, it was not pursued as a time-savings alternative at this juncture.

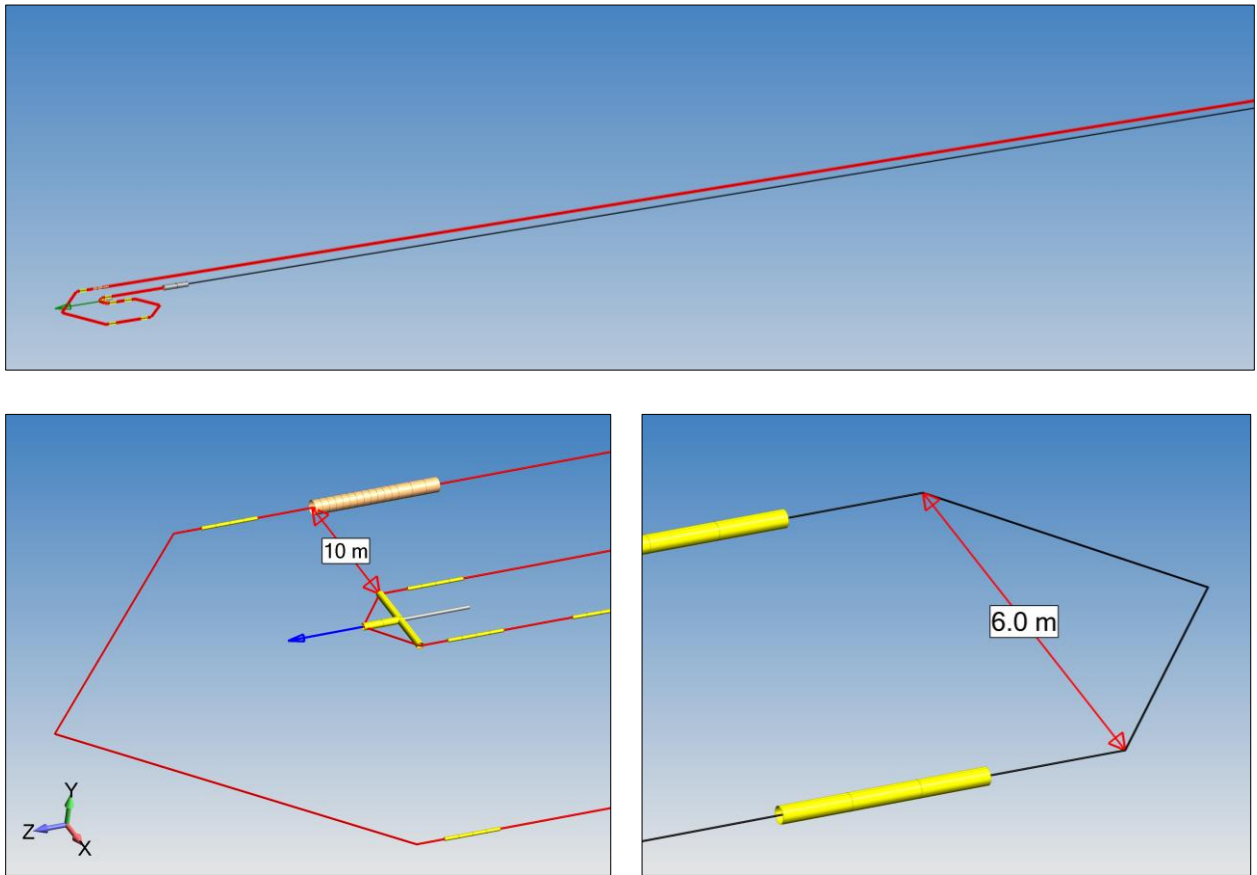


Figure 2 – Preliminary FEA model of heavy-lift rope system

To obtain the smoothest response, a FEA pulley was modeled.

Figure 3 shows the setup. The rope system was tensioned by applying a constant force to the pulley. A spring/damper element was also inserted to smooth-out the dynamic behavior of the rope loop.

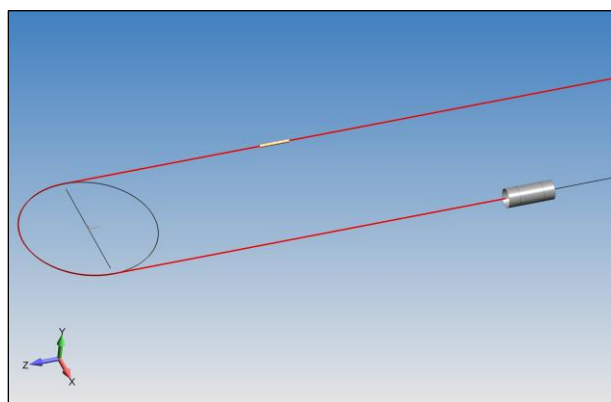


Figure 3 – FEA model of pulley system

Contact (*AUTOMATIC_CONTACT_GENERAL) behavior between the pulley and rope (Beam elements, ELFORM=6) required a bit of fine tuning. The pulley sections were modeled using *MAT_RIGID and to increase the time step while maintaining “contact”, the SOFT=1 option was employed with SOFSCL=0.35. It was a pure Edisonian approach but it worked.

The final model can be termed a racetrack with a tensioned and dampened pulley (ship hoist drum) on one end and fixed pulley on the other end. Although basic in appearance the model is sophisticated in the methodology used to initially tension the rope prior to the lift and to drive the loaded rope to the surface while pulling the haulback to the sea floor. This model is shown in Figure 4. The rope elements are 2 m in length and the model has a total of 7k elements.

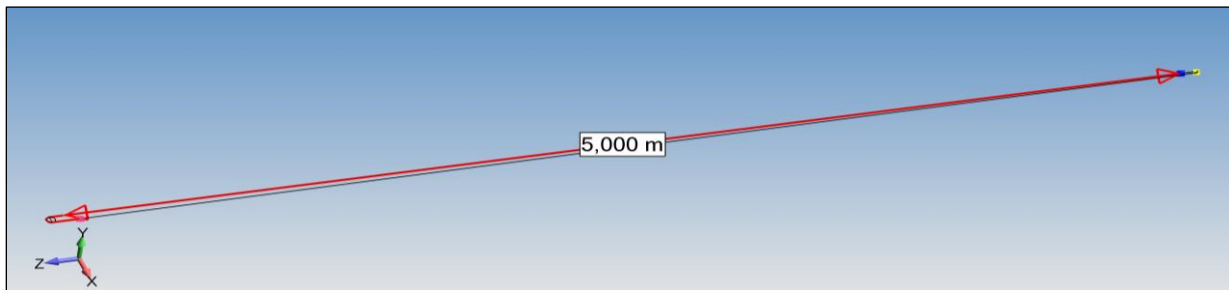


Figure 4 – Heavy-Lift rope system

Fluid Structure Interaction (FSI) Modeling

The hoist system will be submerged in a marine environment and subject to currents that will increase the load on the Dyneema ropes. Furthermore, the interaction of the fluid on the rope will cause flow induced vibration, also known as vortex shedding. To simulate the full coupled effect of fluid flow and a flexible rope system using CFD and FEM would be prohibitively computationally expensive. For this reason, a loose, one way coupling of the fluid flow with a FEM model has been used. This means that the fluid flow effects the rope and payload, but the opposite is not true. This is a reasonable approximation considering the size and mass of the rope in comparison to the fluid.

The general approach is to model the rope and payload using three dimensional rope elements. A rope element is a finite element formulation that only allows tension. No compression or bending is allowed in the element. This is an efficient element formulation and is an excellent representation of the Dyneema ropes. Each rope element has two nodes, and subsequent elements are connected together at their common nodes. Each node in a rope element has three translational degrees of freedom.

To incorporate the effects of the fluid flow on the rope, Predictive engineering has developed an underwater rope fluid structure interaction algorithm (UWCFSI). As the fluid flows over the rope, a pressure difference on the upstream and downstream side of the rope develops as shown in Figure 5. This pressure difference causes a net force that tends to push the rope in the direction of the flow (see Fox *et al.* [4] for more details).

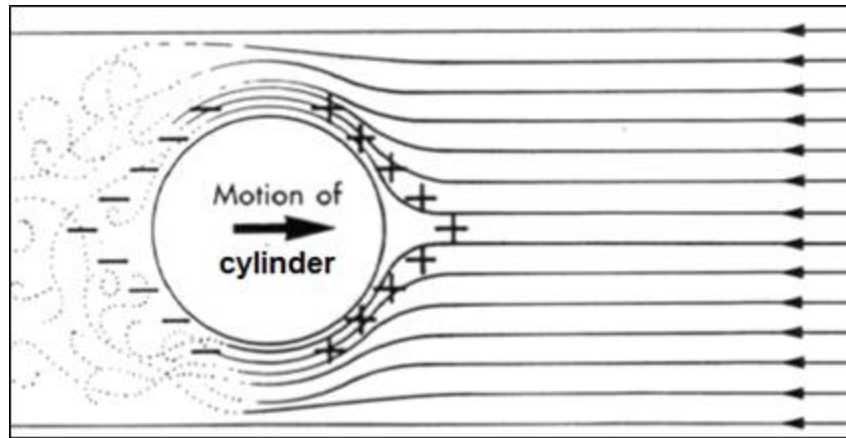


Figure 5 – Fluid flow around an immersed cylinder

The pressure difference has been studied in great detail throughout the years and the resulting force is commonly called a drag force, F_d . The force is proportional to the square of the sea current velocity, $V_{current}$, the density of the sea water, ρ_{sw} , the projected area normal to the flow direction, A_p , and the static drag coefficient, C_d . The basic equation is then:

$$F_d = \frac{1}{2} \rho_{sw} V_{current}^2 C_d A_p \quad \text{Eqn 1}$$

This equation is fine for a one dimensional analysis and quick hand calculations, however, for a 3D FEM code, the velocity of the current must be represented by a vector (with x, y and z directions), as such the drag force is also a vector. Now, since we want to consider the coupling of the fluid with the rope, we must use the relative velocity between the fluid and the rope, $\vec{V}_{Rel} = \vec{V}_{current} - \vec{V}_{rope}$. The drag force vector, \vec{F}_d , equation is now:

$$\vec{F}_d = \frac{1}{2} \rho_{sw} \vec{V}_{Rel}^2 C_d A_p \hat{n}_i \quad \text{Eqn 2}$$

\hat{n}_i is a normalized vector in the direction of the flow. We must use the normal vector to take into account flow in both the positive and negative coordinate directions (otherwise the sign cancels). The normal vector is given by:

$$\hat{n}_i = \frac{\vec{V}_{current_i}}{\|\vec{V}_{current_i}\|} \quad \text{Eqn 3}$$

here, $\|\vec{V}_{current_i}\|$ is the magnitude of the flow velocity. In this sense, if the rope is vibrating in the same plane as the flow, the drag force will have a tendency to attenuate the vibration. Since we are dealing with a collection of finite elements, this equation should be cast into a form that has meaning on a per node basis. So for the i^{th} nodal point, the drag force is:

$$\vec{F}_{d_i} = \frac{1}{2} \rho_{sw_i} \vec{V}_{Rel_i}^2 C_{d_i} A_{p_i} \hat{n}_i \quad \text{Eqn 4}$$

The index is kept for the density and drag coefficient to allow for values that can be a function of depth, direction, temperature, etc. The relative velocity is now:

$$\bar{V}_{Rel_i} = \bar{V}_{current_i} - \bar{V}_{node_i} \quad \text{Eqn 5}$$

where \bar{V}_{node_i} is the velocity of the i^{th} nodal point. Again, for generality, the index is kept for the current since this will allow us to make it a function of depth. Fluid forces are calculated at each node point and are applied to the global force vector in the FEM program. This approach is not a standard feature in LS-DYNA, and because of this, we have developed our own user loading subroutine.

Vortex Shedding

Depending on the importance of the inertia and viscous effects in the boundary layer, vortex shedding can have a significant effect on the forces in the flow directions and transverse to the flow. As the fluid flows around the cylinder, the fluid separates from the surface of the cylinder creating a wake. As the ratio of inertia to viscous forces (Reynolds number) increases, the location of the separation point will oscillate slightly, creating vortices (see Figure 6). The vortices form on one side of the cylinder, detach and then form on the other side of the cylinder. This behavior is typically present when the Reynolds number is greater than ~40 (see Lienart [5]). The Reynolds number is defined as:

$$Re_D = \frac{\rho \|\bar{V}_{Rel}\| d}{\mu} = \frac{\|\bar{V}_{Rel}\| d}{\nu} \quad \text{Eqn 6}$$

The kinematic viscosity, ν is defined as $\nu = \mu/\rho$. As the Reynolds number continues to increase, the frequency at which the vortices are created increases. The various vortex shedding regimes are shown in Figure 7.

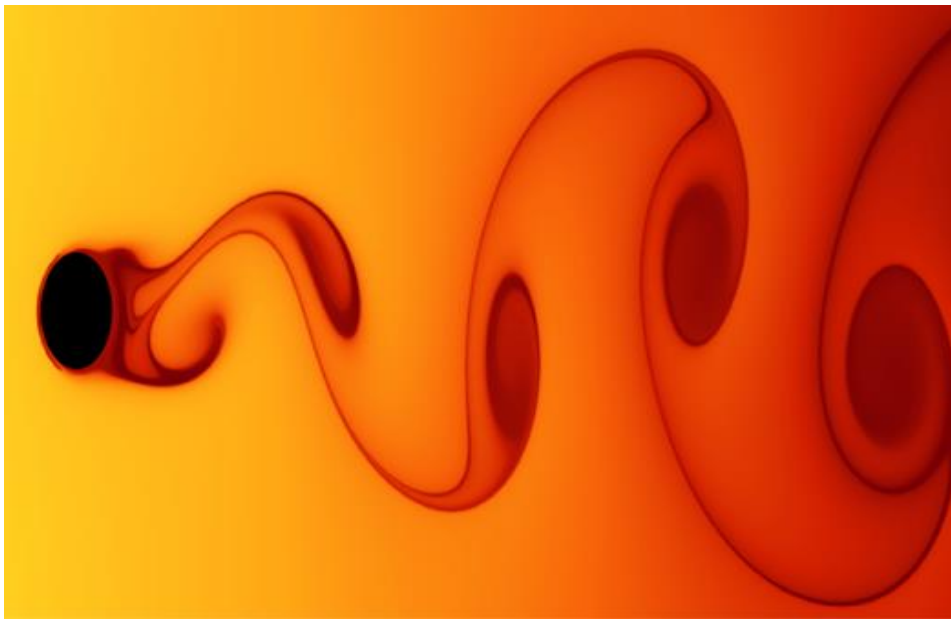


Figure 6 - Vortex shedding

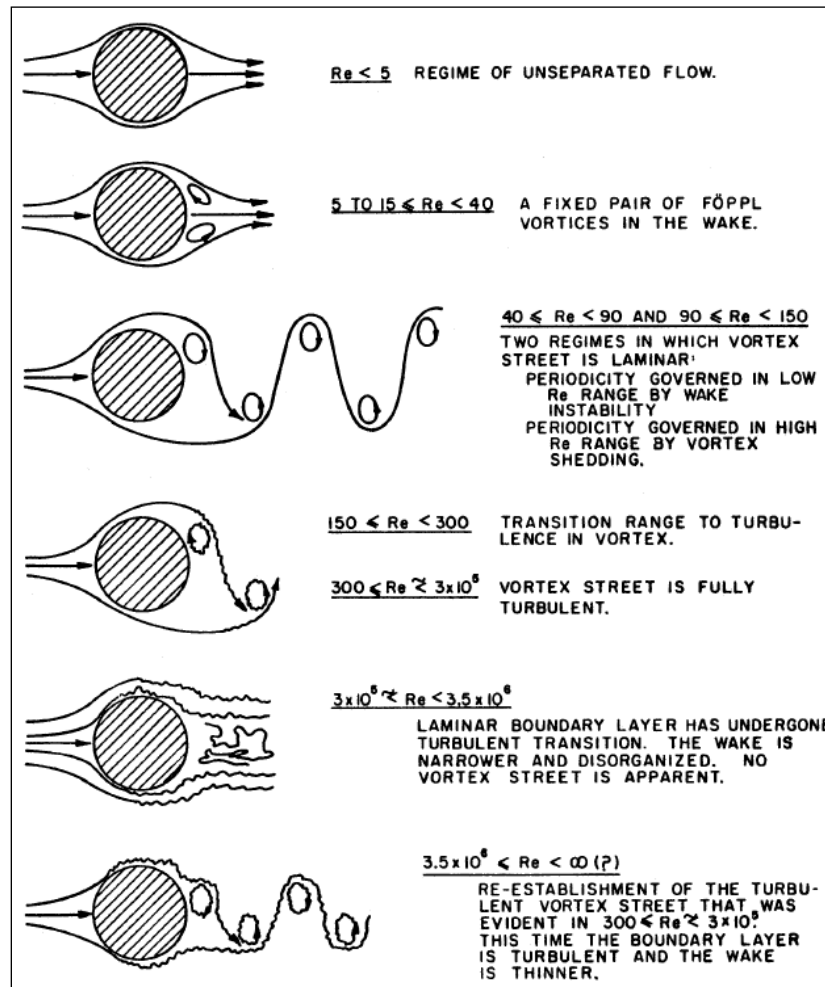


Figure 7 – Vortex shedding regimes

The frequency at which the vortices are created and shed from the surface is called the vortex shedding frequency, f_{vs} , and is a function of the Strouhal number, St , the relative velocity and the diameter:

$$f_{vs} = St \frac{\|\bar{V}_{Rel}\|}{d} \tag{Eqn 7}$$

The value of the Strouhal number depends on Re_D as shown in Figure 8. We can see that the value is ~ 0.2 throughout a large range of Reynolds numbers. On the high side of the envelope is St for a smooth cylinder and the lower side is for a rough cylinder. Since the Dyneema rope will be closer to a rough cylinder, we are able to use $St \approx 0.2$ up to $Re_D \approx 1.0 \times 10^6$. Above this value, St is made to be a linear function of Re_D .

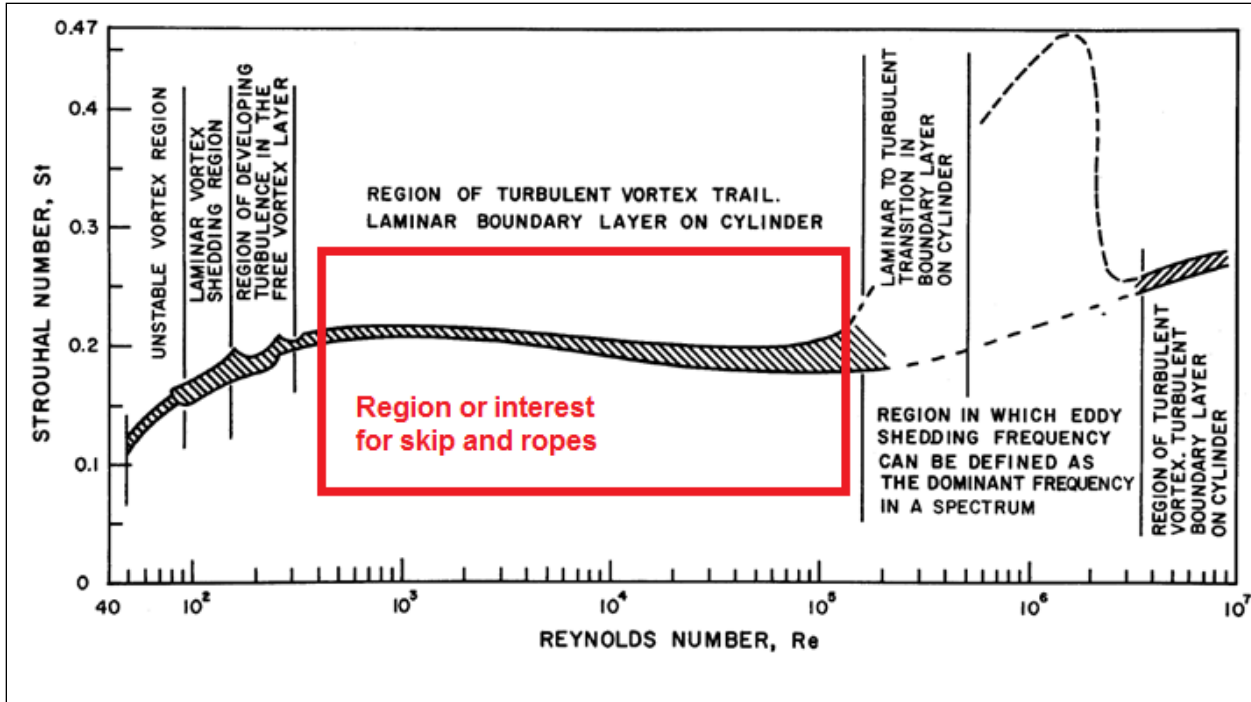


Figure 8 – Dependence of St on Re_D

Considering a typical maximum surface current of ~1 knot (0.514 m/s), the Reynolds numbers for the three main components of the system will be (using kinematic viscosity of sea water $\sim 1.3 \times 10^{-6}$):

- Main Line : $\sim 3.0 \times 10^4$ (subcritical flow)
- Payload : $\sim 1.0 \times 10^6$ (supercritical flow)
- Haul Line : $\sim 1.0 \times 10^4$ (subcritical flow)

From this, we can see that only the payload could be subject to a Strouhal number greater than 0.2. Because the vortices are created in an oscillating fashion on either side of the cylinder, this will cause a force to develop that is transverse to the flow direction (due to pressure variation from one side to the other of the cylinder). This transverse force is akin to a lift force, \bar{F}_{L_i} , and can be taken into consideration in the code by:

$$\bar{F}_{L_i} = \frac{1}{2} \rho_{sw_i} \bar{V}_{Rel_i}^2 C_{L_i} A_{p_i} \sin(2\pi f_{vs}) \hat{n}_{T_i} \tag{Eqn 8}$$

Since the lift force is in the transverse direction to the flow, we determine a normalized vector in the transverse direction based on:

$$\hat{n}_{T_i} = \frac{\bar{V}_{current_i} \times \Delta \bar{x}_{elem_i}}{\|\bar{V}_{current_i} \times \Delta \bar{x}_{elem_i}\|} \tag{Eqn 9}$$

$$\Delta \bar{x}_{elem_i} = \bar{x}_{i+1} - \bar{x}_i \tag{Eqn 10}$$

The lift coefficient, C_{L_i} , will typically be some fraction of the drag coefficient in this case that we will call the vorticity factor, $\lambda_{vs} = C_L/C_d$. The exact value of this factor is not well known, however, we know that vibrations induced by vortex shedding is self-limited (according to Techet [6]). The Lift force can be written as:

$$\bar{F}_{L_i} = \lambda_{vs} \bar{F}_{d_i} \sin(2\pi f_{vs}) \hat{n}_{T_i} \quad \text{Eqn 11}$$

For this reason, λ_{vs} is left as a parameter that can be entered into the user loading subroutine. The magnitude of the oscillation is then limited to one diameter of the cylindrical object in water. We will investigate the rope response for $\lambda_{vs} = 0$ and a maximum value that gives a transverse vibration of one diameter.

The drag force is also affected by vortex shedding; we must now add an oscillatory component, \tilde{F}_{d_i} , to the standard drag force to get a total drag force, \bar{F}_{dTotal_i} (essentially a Fourier series with only the A_0 and A_1 terms):

$$\bar{F}_{d_i} = \frac{1}{2} \rho_{sw_i} \bar{V}_{Rel_i}^2 C_{d_i} A_{p_i} \hat{n}_i \quad \text{Eqn 12}$$

$$\tilde{F}_{d_i} = \tilde{C}_{d_i} \bar{F}_{d_i} \sin(4\pi f_{vs}) \hat{n}_i \quad \text{Eqn 13}$$

$$\bar{F}_{dTotal_i} = \bar{F}_{d_i} + \tilde{F}_{d_i} \quad \text{Eqn 14}$$

\tilde{C}_{d_i} is the dynamic drag coefficient . Note that the excitation frequency of \tilde{F}_{d_i} is twice that of \bar{F}_{L_i} .

User Loading (LOADUD)

Since LS-DYNA does not include such an elaborate approach to simulate the effect of dynamic fluid forces on a rope system, we have developed our own user loading subroutine. We call the algorithm ‘‘Under Water Rope Fluid Structure Interaction’’ (UWCFSI). In order interface with the LS-DYNA code, an object oriented version of the code is required. It can be downloaded from:

<http://ftp.lstc.com/objects/>

(username=objects and password=computer1)

The objects version must be compiled with the appropriate Intel compiler. For the objects version we have worked with, we have used: Intel Parallel Studio XE 2013, which can be obtained from Intel’s archives:

<https://software.intel.com/en-us/intel-parallel-studio-xe>

By default you will be directed to the latest release, however, there will be an option to switch to an archived version (a check box). Make sure to get the correct revision for the objects code (read carefully the readme.txt included when downloading the objects code from the LSTC ftp site).

To activate the UWCFSI algorithm, the LS-DYNA objects library compiled executable must be used for the solver. The name of the executable is: LS-DYNA-SMP-d-R800-UWCFSI-

14012016.exe and was compiled on January 14, 2016 (contact Predictive Engineering for access to the executable). The executable includes Predictive Engineering’s UWCFSI subroutine. The UserLoadingInput.k must be included in the LS-DYNA input deck (containing all the keywords for the structure), this is done by adding:

```
*INCLUDE
UserLoadingInput-14012016.k.
```

Once this is done, the user defined loading subroutine will be called. You should see:

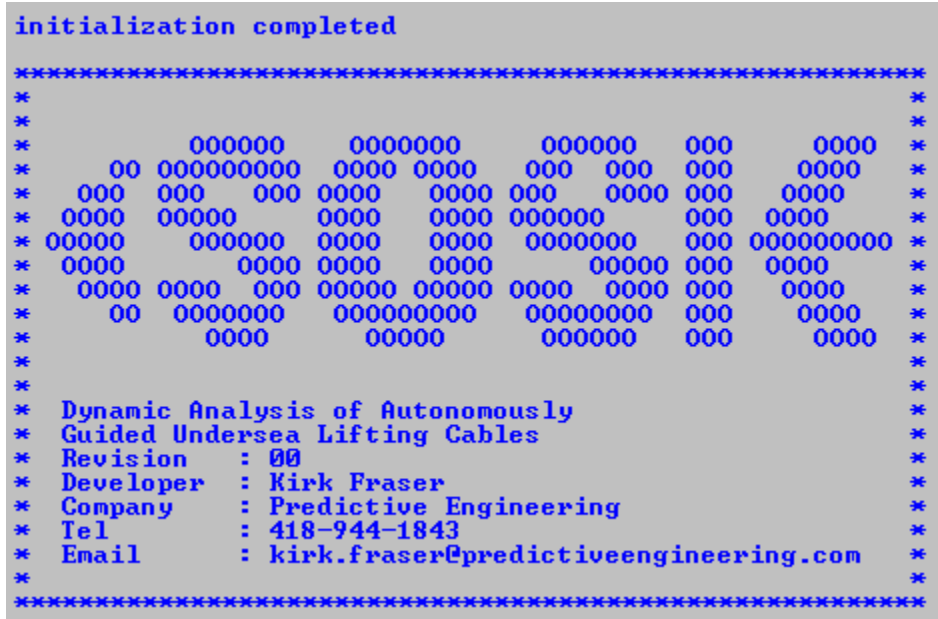


Figure 9 - Callout when UWCFSI is called correctly

If you do not see this at the start of the run, then the solver was not successfully changed.

UserLoadingInput Keyword Description

Card 1	1	2	3	4	5	6	7	8
Variable	VxCrnt1	VyCrnt1	VzCrnt1	VxCrnt2	VyCrnt2	VzCrnt2	Drope	Dhaul
Type	F	F	F	F	F	F	F	F
Remark	1	1	1	1	1	1		

Card 2	1	2	3	4	5	6	7	8
Variable	Dpayload	VertAxis	WTo	WBot	MainLine	PayloadAsn	PayloadDsn	HaulLine
Type	F	I	F	F	I	I	I	I
Remark				2				

Card 3	1	2	3	4	5	6	7	8
Variable	tRamp	ViscK	StNum	VortFac	VelMeth	CdragS	SkpNdA	SkpNdD

Type	F, I	F	F	F	I	F	I	I
Remark	3		4	5	6			

Card 4	1	2	3	4	5	6	7	8
Variable	VskpMeth	Vskp	tRampSkp	Cdyn	CdragL	CdragA	RhoW	CrntSplit
Type	I	I	F, I	F	F	F	F	F
Remark	7	7						1

<u>Variable</u>	<u>Description</u>
VxCrnt1	Velocity of sea current in x direction from WTop to CrntSplit (Remark 1)
Vy Crnt1	Velocity of sea current in y direction from WTop to CrntSplit (Remark 1)
Vz Crnt1	Velocity of sea current in z direction from WTop to CrntSplit (Remark 1)
VxCrnt2	Velocity of sea current in x direction from CrntSplit to WBot (Remark 1)
Vy Crnt2	Velocity of sea current in y direction from CrntSplit to WBot (Remark 1)
Vz Crnt2	Velocity of sea current in z direction from CrntSplit to WBot (Remark 1)
Drope	Diameter of the main line
Dhaul	Diameter of the haul back line
Dpayload	Outer diameter of the payload
VertAxis	Orientation of the vertical axis = 1 : x-axis = 2 : y-axis = 3 : z-axis
WTop	Vertical coordinate of the location of the top level of water
WBot	Vertical coordinate of the location of the bottom level where the current can be considered to be zero
MainLine	Part number of the main line
SkpAsnd	Part number of the ascending payload (see Remark 2)
SkpDsnd	Part number of the descending payload (see Remark 2)
HaulLine	Part number of the haul line
tRamp	> 0 : Ramp up time for the fluid forces, assumed to have no fluid forces at time zero and ramp up to full fluid forces at time = tRamp (see Remark 3) < 0 : Defines the load curve to apply the fluid forces
ViscK	Kinematic viscosity of the sea water (used to calculate the Reynolds number)
StNum	Strouhal number (typically assumed to be ~0.2) (see Remark 4)
VortFac	$\lambda_{vs} = C_L/C_d$ (see Remark 5)
VelMeth	Method for applying fluid forces in UWCFSI code (see Remark 6) = 0 : Use $\bar{V}_{Rel_i} = \bar{V}_{current_i} - \bar{V}_{node_i}$ (provides realistic fluid forces and incorporates fluid damping) = 1 : Use $\bar{V}_{current_i}$ (only the sea current is used, only for academic

	interest, not realistic, does not incorporate any fluid damping)
CdragS	Drag coefficient on the fairing of the payload
SkpNdA	Nodal point number for topmost node on the ascending payload (represents the fairing)
SkpNdD	Nodal point for bottommost node on the descending payload (represents the fairing)
VskpMeth	Method for considering the vertical velocity of the payload (see Remark 7) = 0 : Use Vskp = 1 : Use the calculated velocity of the payload
Vskp	Towing velocity of the payload (see Remark 7) > 0 : Ramp up time for the fluid forces on the blunt face (fairing) of the payload ascending or descending in the water (due to Vskp), assumed to have no fluid forces at time zero and ramp up to full fluid forces at time = tRamp (see Remark 3) < 0 : Defines the load curve to apply the fluid forces to the payload fairing
tRampSkp	
Cdyn	Dynamic drag coefficient that applied to the drag force (in direction of fluid flow)
CdragL	Drag coefficient in the lateral direction on the main and haul line (~1.0 for a rope)
CdragA	Drag coefficient in the axial direction on the main and haul line (~0.1)
RhoW	Density of the sea water (~1025 kg/m ³)
CrntSplit	Elevation at which the current changes (assuming a two level current (Remark 1))

Remarks

1. The sea current is defined in the global coordinate system; in this manner any sea current direction can be considered. The current is considered to be split into two zones, VCrnt1 and VCrnt2 that act from WTop to CrntSplit and CrntSplit to WBot respectively. The total sea current will be $V_{current} = \sqrt{V_{x_{current}}^2 + V_{y_{current}}^2 + V_{z_{current}}^2}$
2. A minimum elevation level is included to allow the code to be parametric and to take into account the eventuality that the client might like to investigate zero current at the sub-sea level
3. The ramp time is used to ramp up the fluid forces from time zero. This is done to limit the dynamic effects. Applying the fluid forces to abruptly will have a tendency to over excite the system. It is assumed that the payload is not moving during this ramp up time
4. The Strouhal number can typically be assumed to be ~0.2 across a wide range of Reynolds numbers for a rough cylinder
5. The vorticity factor should not be above 1.0, this would mean that $C_L > C_d$, which is non-physical for a cylinder. A reasonable limit on this factor will be such that provides a transverse rope vibration magnitude of less than one rope diameter
6. Using VelMeth = 1 is non-physical, but can be used to verify that the fluid forces are being applied in the same manner as *LOAD_NODE

7. No default values are included in the subroutine, the user is warned against leaving a field blank

The vertical velocity of the payload used in the drag calculation can be taken from the dynamic behavior of the payload ($V_{skpMeth} = 1$) or it can be assumed to be the same haul speed ($v_{skpMeth} = 0$, drag force calculated using V_{skp})

Utility of Interactive Dynamic Analysis of Heavy-Lift Subsea Ropes

Given the economic importance of this work for our client, a sensitivity study was done to see if it was possible to trigger harmonic excitation (e.g., strumming) in the rope system during a heavy lift. Results showed that the lift system was dynamically stable on a variety of operating conditions where sea currents were varied and additionally when the ship side winch was assumed to move in a harmonic fashion to simulated various sea states. Figure 10 shows an example of how the rope is pushed around by currents during a heavy-lift operation. Each image is a snapshot at a different depth from the sea floor bottom. The left-hand side of each image is toward the surface.

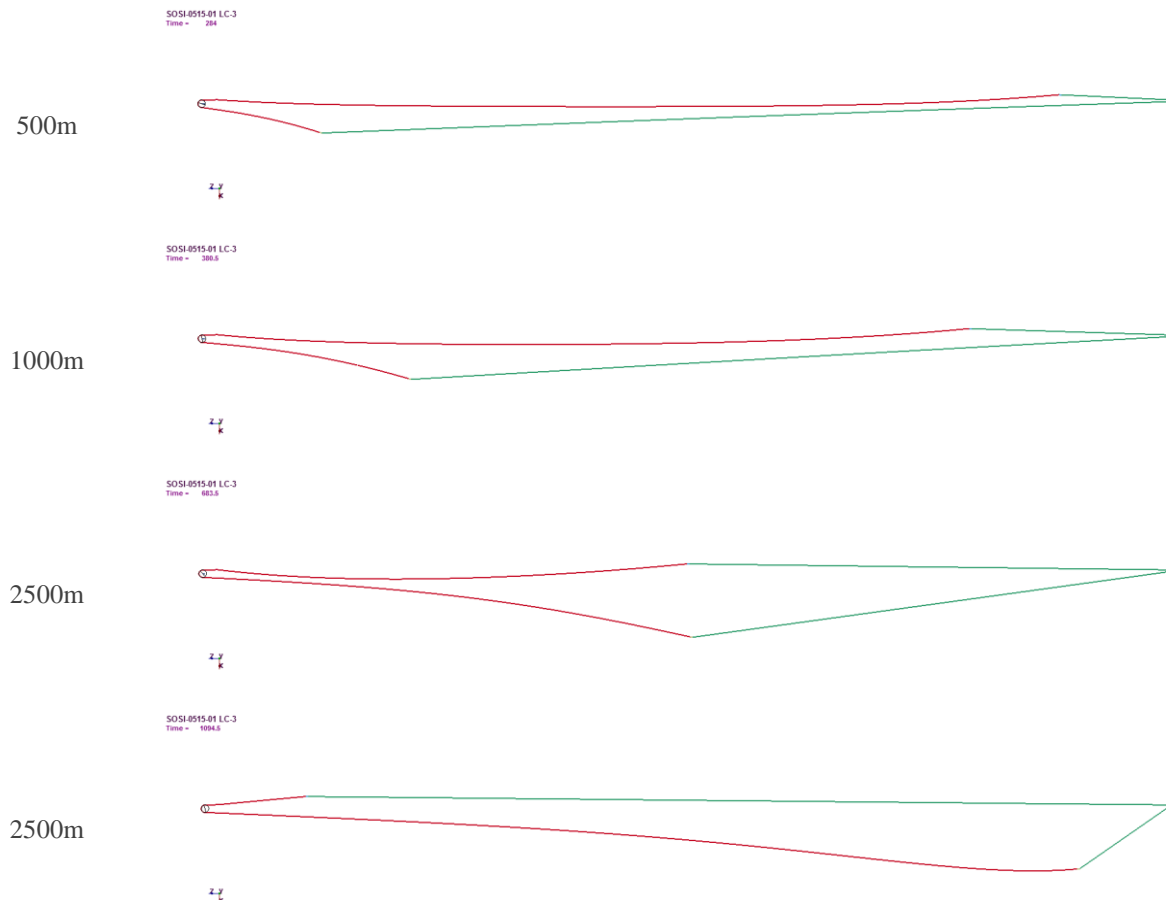


Figure 10 – Example of rope movement during heavy-lift from sea floor

And of course, of major interest was the possibility that the rope may cross during lifting due to an un-favorable combination of current, lift speed and cargo weight. Figure 11 shows what can happen with the rope crossing lines at a depth of 2500m.

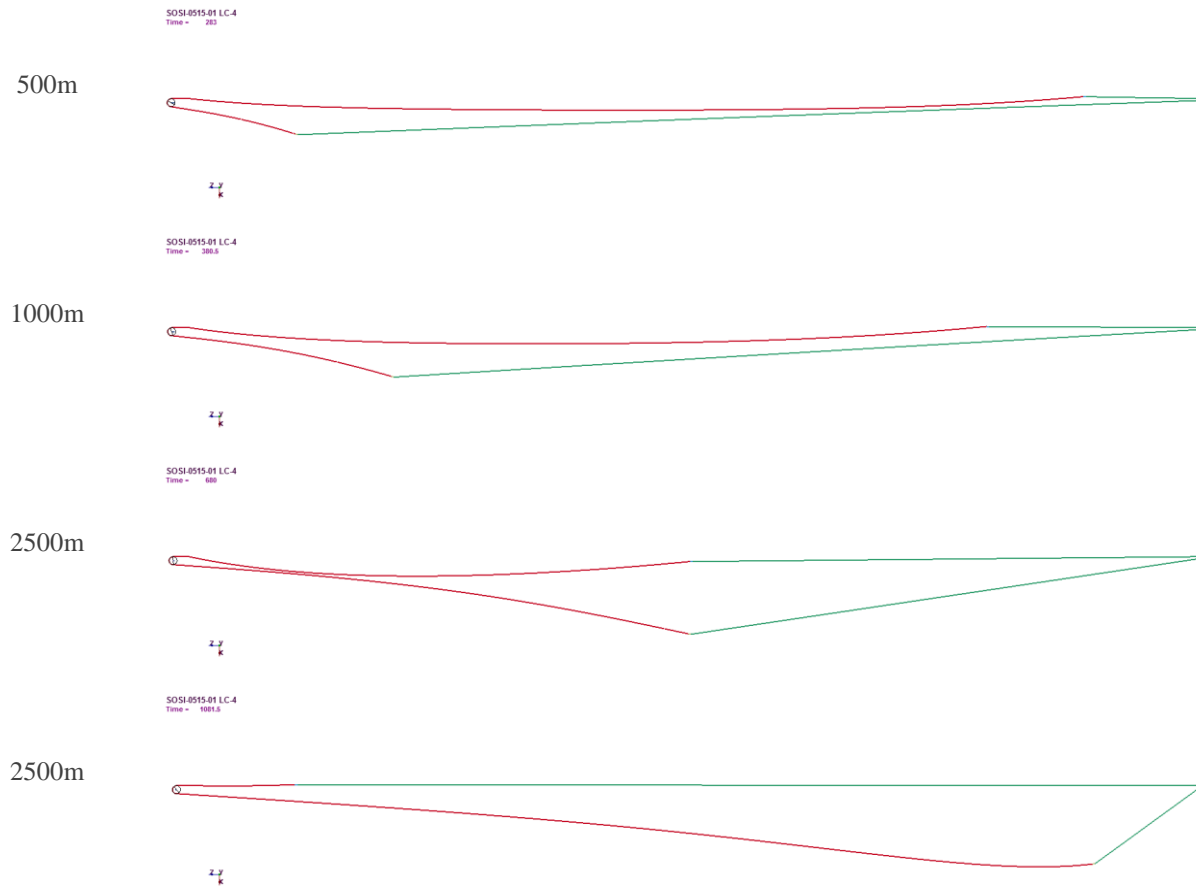


Figure 11 – Example of rope crossing during heavy-lift from sea floor

One of the advantages of building the model using LS-DYNA is the ability to extract rope stresses and winch forces through-out the lift operation. This was very useful in assessing the axial loads on the plastic haulback and mainline ropes. Figure 12 shows a representative plot of the rope forces during heavy-lift. The top image is at calm seas while the bottom plot is at a hypothetical sea state 3. Although the bottom image shows oscillation during lift, it was driven by the movement of the ship and did not overly excite to the extent that it would cause rope damage.

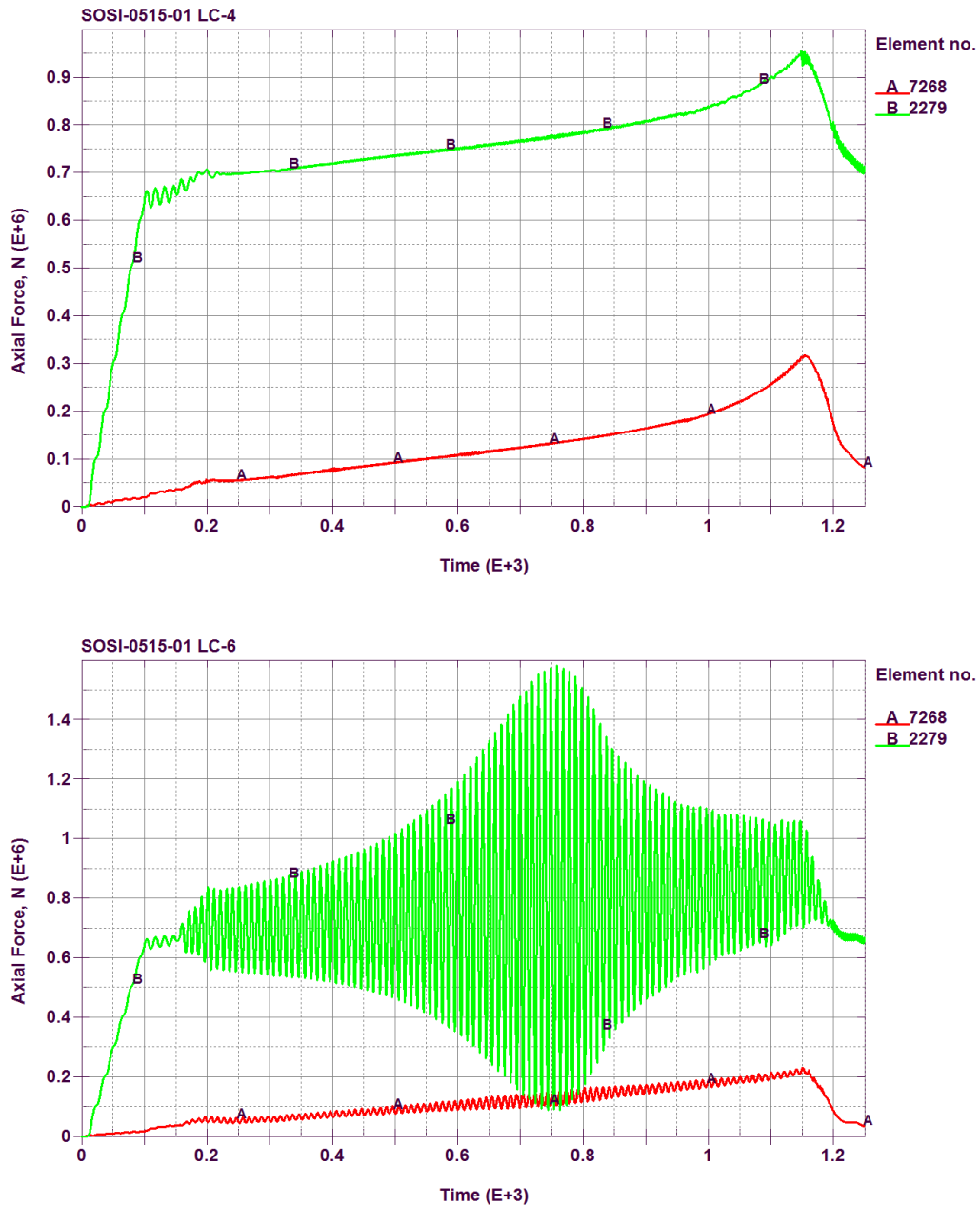


Figure 12 - Haulback (B) and mainline (A) rope axial forces during heavy-lift

Summary

An elegant method was shown to simplify a FSI problem to a numerically quick solution that easily facilitates the exploration of dozens of variables.

The key developments of this work are:

- Idealization of vortex shedding and fluid drag forces to a set of simple equations;
- Development of the loadud user routine that interactively applies idealized fluid forces to the rope;
- Coupled transient dynamic analysis of a rope system;
- And importantly, a FSI solution that runs in minutes and explores dozen of designs variables to be explored in a matter of days.

Going Forward

The authors see this technique as pictorially shown in Figure 13, having broad applications to wave action against flexible or rigid structures or wind gusts against dynamic structures and of course the wide open ocean.

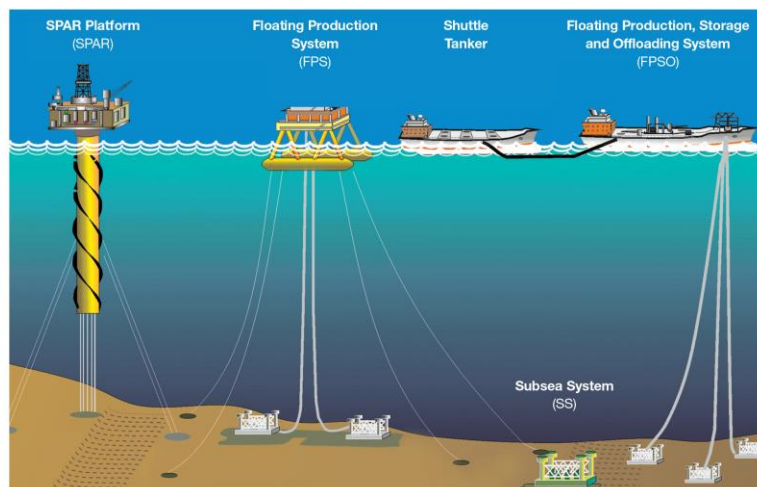


Figure 13 – Examples of fluid structure interaction where the LS-DYNA LOADUD is possible

Acknowledgements

The authors wish to thank the gracious and ever resourceful technical staff at LSTC and DYNAmore for helping us with this project; without their thoughtful suggestions and assistance this project would have taken months longer.

References

- [1] Laura PA, al. e. A survey of Publications on Mechanical Ropes and Rope Systems. Washington DC: Institute of Ocean Science and Engineering, the Catholic University of America; 1968.
- [2] Hafen BE, al. e. Rope Strumming Suppression. Naval Facilities Engineering Command, Program No YF5255609101201B. 1977.
- [3] Fritz RJ, al. e. The Vibration Response of an Annular Fluid on the Vibrations of a Long Rotor, Part 1 – Theory; and Part 2 – Test. J Basic Engineering, Trans ASME. 1970;92.
- [4] Fox RW, McDonald AT, Pritchard PJ. Introduction to fluid mechanics. 6th ed. New York: Wiley; 2004.
- [5] Fraser K, St-Georges L, Kiss LI. Hybrid thermo-mechanical contact algorithm for 3D SPH-FEM multi-physics simulations. 4th International Conference on Particle-Based Methods. Barcelona Spain2015.
- [6] Techet AH. Vortex Induced Vibrations - Lecture 13.42. MIT2005.